Basic Investigation of Fluid-Acoustic Interactions in a Supersonic Rectangular Jet Ejector

FINAL REPORT ON NASA GRANT NAG 1-1497

Submitted to

NASA Langley Research Center
Hampton, VA

by

The Department of Mechanical Engineering
FAMU/FSU College of Engineering
Florida State University
Tallahassee, FL

Professor Anjaneyulu Krothapalli
Principal Investigator

An On-line PIV Study of a Rectangular Supersonic Jet Ejector Flow-Field

C.B. Ross*, A. Krothapalli†, and L.M. Lourenco‡
Department of Mechanical Engineering
Florida A&M University and Florida State University
Tallahassee, Florida 32316

Abstract

The internal mixing region of a small-scale supersonic rectangular jet ejector was experimentally investigated. A rectangular converging-diverging nozzle (AR=4) with a design Mach number of 1.5 issues into a constant-area rectangular duct. A physically realistic duct-to-jet area ratio of 2 was used for all experiments, resulting in secondary fluid entrainments approaching M_2=0.6. Particle Image Velocimetry (PIV), flow visualization, and surface pressure measurements were used to study the internal characteristics of the ejector flow-field. Substantial mixing increases were observed when the most unstable Strouhal frequency of the unheated primary jet is matched with a transverse duct mode of the ejector. This self-excitation resulted in the production of large-scale structures between the primary and secondary streams. Specifically, the presence of this effect in an unheated case resulted in a 13% increase in secondary mass entrainment and thrust augmentation above the expected performance trends. With the exception of the self-excited case, the growth rates of the internal mixing layers agree very well with published planar mixing-layer data. This indicates that the strong static pressure gradient in the duct has a negligible effect on mixing. However, the growth rate of the self-excited mixing layer exceeded the growth rate measured in a planar free shear layer by over 50% (measured at identical convective Mach numbers). Finally, the primary jet was heated to 650 K to study the temperature effects on internal mixing and performance. The increased density and velocity ratio in the heated case resulted in improved mixing, fluid entrainment, and thrust augmentation.

1.0 Introduction

The work presented here is part of an ongoing research program to develop supersonic jet noise reduction techniques for application to the High Speed Civil Transport (HSCT). The use of an ejector in conjunction with a multi-lobed or mixer nozzle is considered to be a promising concept that meets the noise abatement requirement.[1] Much of the earlier work dealt mainly with high area-ratio ejectors (duct area/primary nozzle exit area) in order to provide thrust augmentation for V/STOL aircraft.[2,3] In the current application, the ejector device must be compact and provide significant noise reduction without any detriment to high-speed aerodynamics. It has been established that a fluid-acoustic interaction inside the ejector, through the modification of the mixing region, plays a significant role in the radiated noise characteristics of the jet.[4] When the most amplified instability mode of the primary jet was matched with one of the duct modes, enhanced mixing between primary and secondary streams inside the ejector duct was observed by Hsia et.al.[5] Additionally, significant far-field noise reductions were observed for small area-ratio (< 4) ejectors.[6] However, a thorough knowledge of the mixing region inside the ejector, much less its relationship to the radiated noise field, is still not available. The purpose of this investigation was to obtain the detailed characteristics of the mixing region of the ejector flow by the use of Particle Image Velocimetry (PIV), conventional flow visualization, and pressure measurements.

The primary role of an ejector is to entrain and mix large amounts of secondary cold air with a hot primary jet within the shortest possible duct length. As a result, the jet centerline velocity prior to exhausting into the surrounding atmosphere is reduced. This, combined with

*Assistant in Research, Member AIAA.

† Fuqua Chair, Professor, and Associate Fellow AIAA.

‡ Professor, Member AIAA.

the natural shrouding effect of the ejector side walls, has shown promise as a valid noise suppression device. In addition, the entrainment and acceleration of cold ambient air results in a desirable net thrust augmentation relative to the free jet alone.

The presence of a high-velocity secondary stream in the ejector duct typically inhibits the mixing of the primary jet (in comparison to the equivalent free jet). In previous studies, many passive techniques have been used to promote mixing between the two streams. Typically, these involve some alteration of the primary jet nozzle exit geometry. While improvements in mixing were made, many of the approaches resulted in significant thrust losses which negate the thrust augmentation derived from the ejector (e.g. the 20% thrust loss "tube jet" of 1968). We propose that the fluid-acoustic interaction can be harnessed to increase the mixing rate without any additional loss of thrust in the primary nozzle. Such fluid-acoustic interactions inside the ejector have been observed to increase the mixing over the base ejector, thereby reducing the required shroud length while retaining the overall performance.[7]

Based on past experimental observations, the ejector flow features depend strongly on the following parameters: exit geometry of the primary nozzle, the mixing duct geometry, ejector/nozzle area ratio, primary jet pressure and temperature, primary jet Reynold's number, and the forward flight Mach number. In the present investigation, a convergent-divergent rectangular nozzle was used for the primary nozzle. The ejector shroud consisted of a convergent inlet followed by a constant area duct. The range of operating parameters is described in the next section.

2.0 Experimental Facility

All measurements were made in the blow-down jet facility of the Fluid Mechanics Research Laboratory (Fig.1). The air is supplied by a collection of storage tanks (10 m^3 total volume) containing air pressurized to a maximum of 13.8 MPa. The series of digitally controlled electrical heaters (450 kW total heating power) are capable of increasing the primary jet stagnation temperature to 750 K (±2 K). A series of digitally-actuated control valves are able to maintain a constant supply pressure to the primary jet over the operational range of 0-1.0 MPa (±5 kPa).

This ejector study was conducted using a rectangular converging-diverging primary nozzle issuing into a rectangular duct (Fig.2). The nozzle was designed for an exit Mach number of 1.5 and has a short dimension height H=10.7 mm and width W=42.8 mm. The entrance region of the duct has a smooth aerodynamic shape for minimal inlet losses. The duct dimensions (width W_1 = 47 mm, height H_1=32 mm, and length L=164 mm) were optimal, based on previous acoustic tests that involved a variable area-ratio ejector.[6] The ejector duct was constructed with borosilicate windows in each of the four side walls for flow-visualization and PIV measurements of the internal flow. The window design allowed an unobstructed view of the entire long dimension and all but 1 mm of the short dimension (viewing the XY plane). The top window section can be replaced by an aluminum plate containing 30 surface static pressure taps, with the tap locations spanning from the contoured leading edge to the duct exit.

The surface static pressure along the center of the ejector was recorded directly from a Wallace and Tiernan 0-15 psig digital transducer via a Scanivalve system connected to the 30 surface ports. Pitot pressure surveys of the high-speed flow were conducted and recorded using standard procedures and instrumentation. A conventional 'Z'-type schlieren system with a 30 cm field-of-view was used to visualize the ejector flow-field. The strobe source has a flash duration of about 1 μs. The image was captured on a high resolution (1280x1024 pixel) Kodak Model 1.4 Megaplus video camera and recorded in digital form on a Microway 486 PC compatible.

For PIV measurements, the primary jet was seeded with commercially available 0.3-0.8 μm Al_2O_3 powder particles. The particles were introduced by a mechanically agitated, solid particle generator [8]. Undesirable large particle agglomerates were removed using a cyclone separator with an adjustable cut-off size. The secondary ambient flow entering the ejector was also seeded using the same system. The tracer particles were illuminated by high intensity (100 mJ/pulse) laser sheets produced by a dual Spectra-Physics Nd-YAG laser system (see Ref.9). The pulse duration was about 10 ns, while the pulse separation was about 1 μs. The laser sheet, 10 cm wide

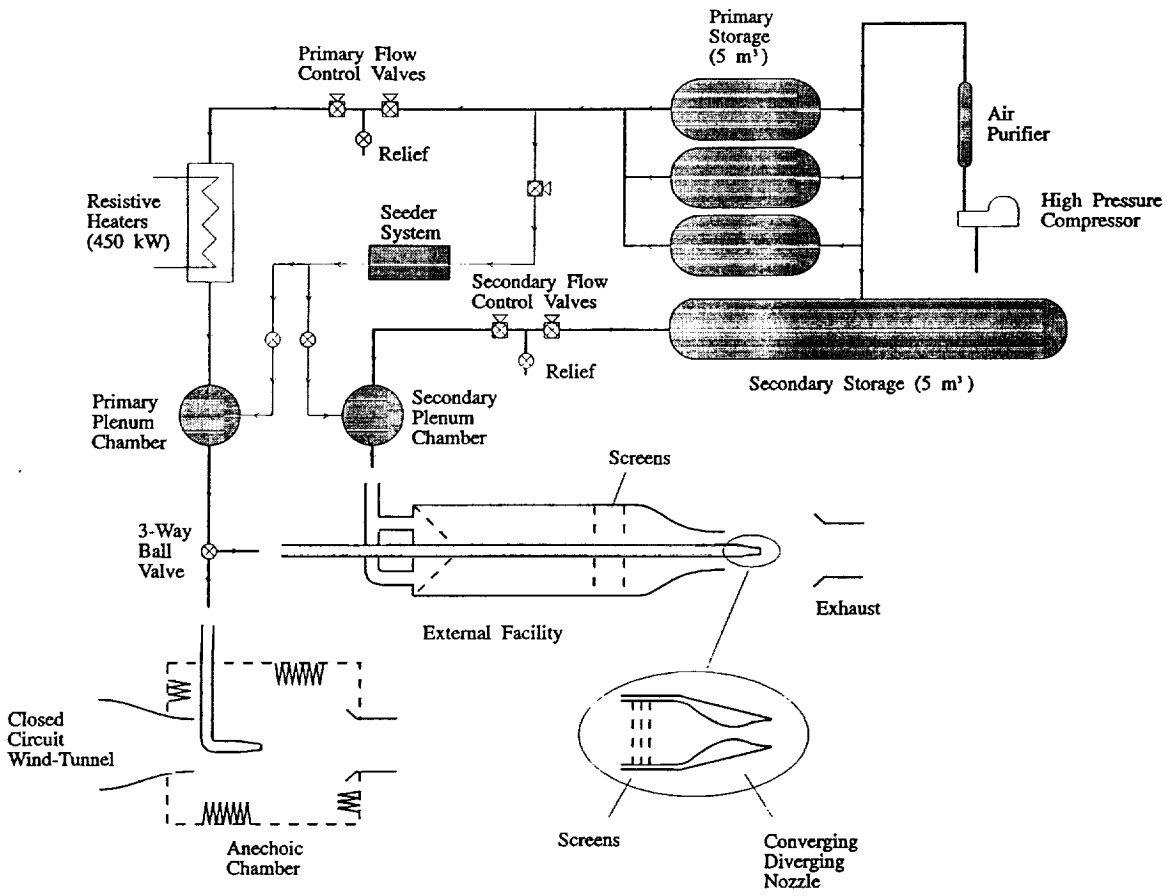

Fig.1 High-speed blow-down jet facility.

and 1 mm thick in the test section, was produced using a standard combination of spherical and cylindrical lenses. The laser sheet was positioned to illuminate the XY plane along the center of the jet axis, allowing analysis of the predominately two-dimensional flow in the short dimension of the ejector. A Kodak 4.0 MB (2000 x 2000 pixel) CCD camera was used to acquire double-exposed images of the flow field. An IBM RISC 6000 Unix workstation running FFD MKIV "On-Line" PIV software was used to acquire and analyze the double exposed images. For details of the PIV technique, reference can be made to Lourenco et al[9]. To resolve the large dynamic range of the velocity measurement, a high-speed (6,000 rpm) rotating mirror system was used to add a positive bias shift to the second image prior to recording[10].

In order to clarify the free-jet and ejector-jet comparisons made in this paper, the parameteric definitions are reviewed here. In studies involving supersonic free-jets, the fundamental parameter used for comparison is the pressure ratio (R), defined as the nozzle stagnation pressure divided by the ambient pressure at the nozzle exit ($R=p_{01}/p_{amb}$). In the ejector, the pressure at the nozzle exit is considerably lower than ambient pressure due to the induced high-velocity secondary flow. Therefore, the Nozzle Pressure Ratio is defined with respect to the local nozzle exit pressure in the ejector as $NPR=p_{01}/p_2$, where p_2 is the static pressure measured at the jet exit. By using this definition of NPR, the ejector flow-field can be compared to an equivalent free-jet flow-field with both nozzles operating at the same expansion condition.

In both ejector cases and free-jet cases, the nozzle stagnation pressure was varied over the range $R= p_{01}/p_{amb}$ =2.0-5.0 at several temperatures ratios between $\theta= T_{01}/T_{amb}$ = 1.0-2.5. The jet exit Reynolds number (based

on short dimension height) varied from 0.8-3.2x10^5. All flow quantities were measured in a coordinate system having its origin at the center of the nozzle exit (referring to Fig.2).

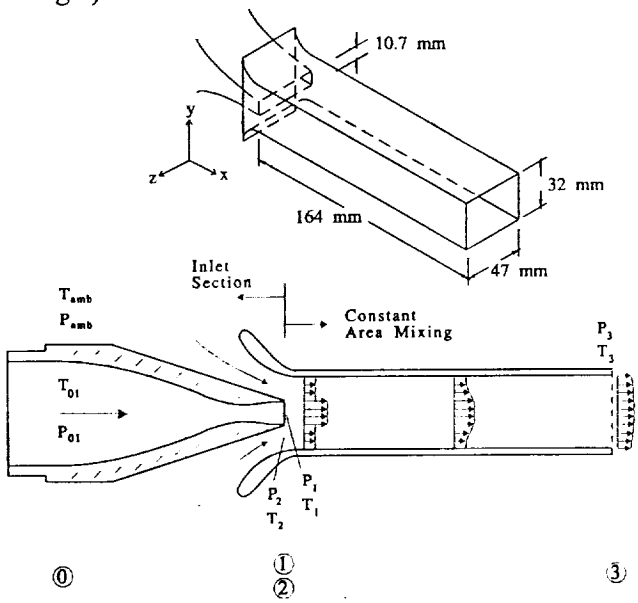

Fig.2 Ejector model and coordinate system.

As shown in the following sections, the unheated NPR=3.4 case was singled out for study because it corresponds to the nozzle pressure ratio where the maximum resonance is occurring in the ejector. The unheated NPR=3.7 case is used as a reference case in which resonance is not detectable. Despite the large variation in ejector performance between these cases, the primary nozzle is nominally operating at design conditions for M=1.5 at both pressure ratios. This allows the comparison to the corresponding ideally-expanded free-jet.

3.0 Results and Discussion

3.1 Aerodynamic Measurements

In order to provide an indication of the internal flow development, the static pressure along the centerline of the ejector duct surface was measured. This measurement was made at several pressure ratios with an unheated primary jet (θ =1.0). Figure 3 depicts the normalized surface pressure variation $C_p = (p_{surf}-p_{amb})/p_{amb}$ along the centerline of the duct for two selected nozzle pressure ratios (NPR=3.4, 3.7). The rapid static pressure decrease in the inlet section indicates an acceleration of fluid into the duct entrance. In the region following the duct entrance, the mixing process results in an increase in C_p with the streamwise direction. For the NPR=3.4 case, one observes a change in the slope of this curve at the axial position x/h=11 which may indicate rapid mixing in this region. Although not plotted here, the static pressure curves obtained at all other pressure ratios were very similar in character to the NPR=3.7 case.

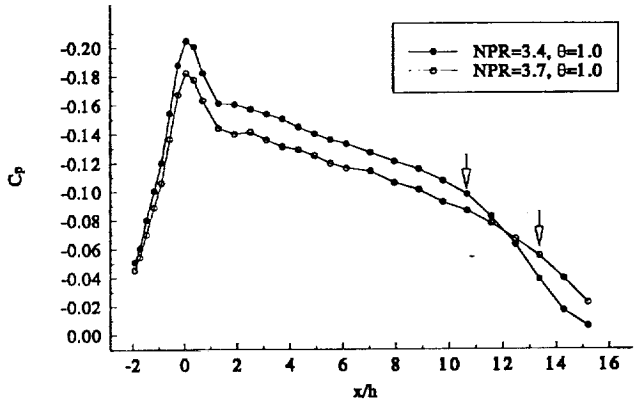

Fig.3 Interior surface pressure along the centerline of the ejector duct.

The minimum surface static pressure measured at the duct entrance ($C_{p,min}$) is generally a good indicator of the entrainment performance of the ejector. When $C_{p,min}$ is plotted in Fig.4 as a function of the primary jet pressure ratio R, a monotonic decrease is observed in the unheated case until the pressure ratio NPR=3.4 is reached. At this point, a sudden deviation from the expected trend is seen, suggesting a change in the mixing processes occurring inside the ejector. However, the heated jet ejector case (θ =2.2) exhibits a smoother decrease in $C_{p,min}$ with respect to increasing R, without the strong deviation seen in the unheated case. To clearly see the variation in performance in the unheated case, the mass entrainment performance was calculated from isentropic relations and the static pressure at the duct entrance. The secondary mass flow is

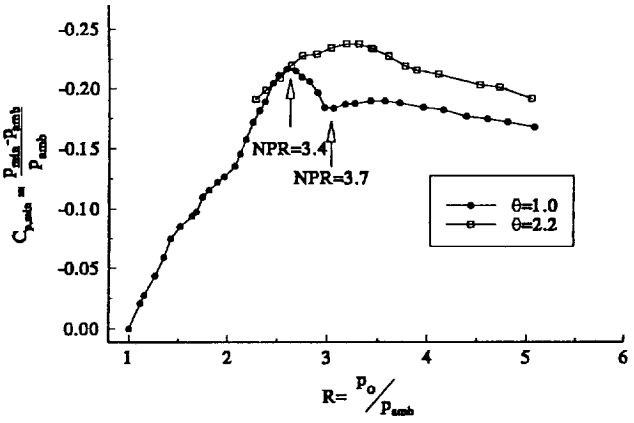

Fig.4 Minimum static pressure at ejector duct entrance.

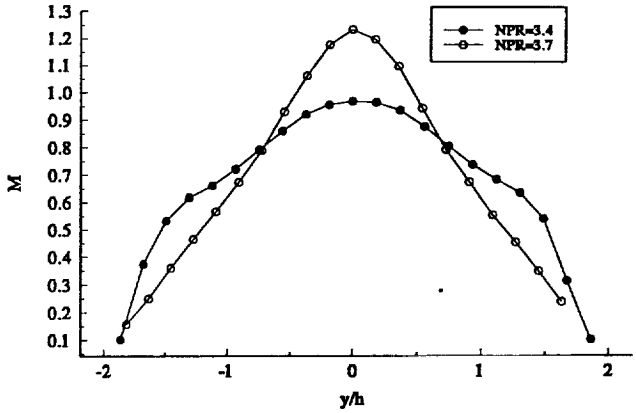

Fig.6 Mach number profile in XY plane of ejector exit for selected unheated (θ=1.0) pressure ratios.

normalized by primary jet mass flow (m_2/m_1) and plotted with respect to R in Fig.5. With this proper normalization, the deviation from expected trends is clearly seen in the unheated case where a 13% entrainment improvement occurs at NPR=3.4 over the solid line. The solid lines indicate a trend of decreasing performance with increasing primary jet pressure ratio, a general trend of ejectors well documented by previous investigators [11].

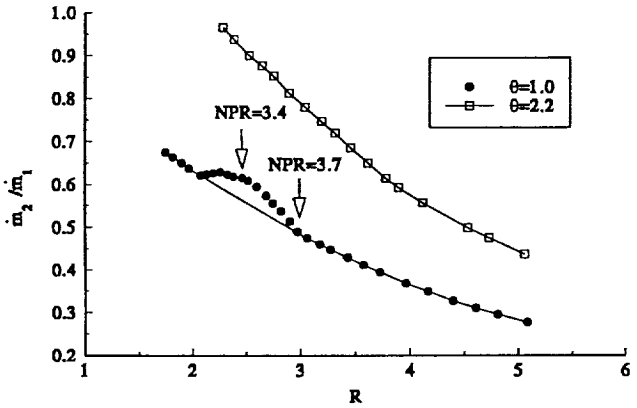

Fig.5 Mass entrainment performance of ejector.

Mach number profiles were obtained at the ejector duct exit from pitot measurements in the XY plane in order to give an indication of the mixing within the ejector. Figure 6 shows profiles at x/H=16 spanning the short dimension at a temperature ratio of θ =1.0 and pressure ratios of NPR=3.4 and 3.7. In comparing the two cases, the fuller profile in the NPR=3.4 case indicates a considerable improvement in mixing when compared to the NPR=3.7 case. In essence, the Mach number profiles indicated a relative lack of mixing at all temperatures and NPR's tested with the exception of the unheated NPR=3.4 case shown.

The thrust augmentation of the ejector shroud was estimated by integrating the surface static pressure on the inlet section in a direction parallel to the jet axis (see Fig.7). This pressure force was normalized by the calculated primary jet thrust, including primary-jet corrections for off-design operation [12]. As can be shown by performing a momentum balance, the overall thrust augmentation of the jet-ejector combination over that of the primary jet can be attributed to the suction pressure on the inlet section. Except in the vicinity of NPR=3.4, the

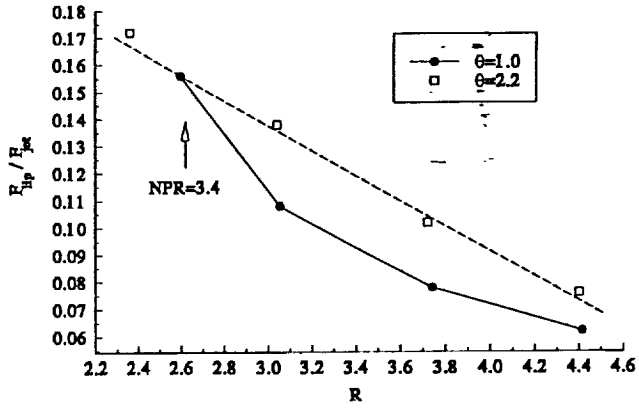

Fig.7 Thrust augmentation of ejector due to inlet pressure force.

thrust augmentation performance of the cold ejector is much less than the corresponding heated jet ejector. These observations are in accordance with one-dimensional isentropic theory [13].

In a previous study of same jet ejector by Krothapalli et al.[4], the near-field sound spectra were investigated to determine the relationship between the acoustic and aerodynamic performance of the unheated jet ejector. It was found that a strong acoustic resonance was present in the duct at NPR=3.4, and the dominant discrete frequency of 5.5 kHz matched the first calculated transverse mode of the ejector duct. It was also discovered that the Strouhal number corresponding to this pressure ratio falls within a range of the unstable St numbers characteristic of cold rectangular jets. Thus, the enhanced aerodynamic performance of the unheated jet ejector at NPR=3.4 is a result of fluid-acoustic interactions inside the ejector, quite similar to those discussed by Hsia et al.[5]

3.2 Schlieren Flow Visualization

Figure 8 depicts instantaneous schlieren photographs of the ejector flow-field at NPR=3.4. and NPR=3.7. Figure 8(a) corresponds to the pressure ratio where the resonant self-excitation and associated performance gain is maximized, as inferred from the aerodynamic measurements of Section 3.1 and acoustic results of the previous study [4]. In this case the jet is "flapping" in an antisymmetric fashion. In Figure 8(b), this sinuous motion is not seen at the slightly higher pressure.

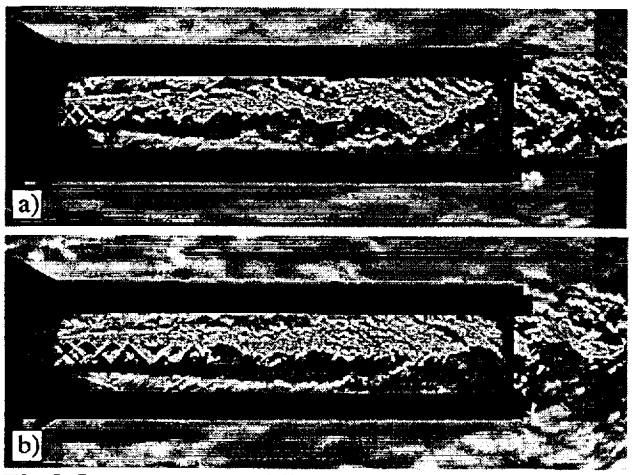

Fig.8 Instantaneous schlieren photographs of unheated ejector flowfields (θ=1.0), a) NPR=3.4 (at resonance), b) NPR=3.7 (no resonance).

To investigate the periodicity of the ejector flow in the NPR=3.4 case, averaged phase-locked schlieren photographs were taken with the strobe synchronized to the most dominant frequency of f=5.5 kHz (see Fig.9). A well-organized sinusoidal motion of the jet is seen propagating in the downstream direction at this resonant frequency. This indicates the staggered production and rapid growth of large structures in the shear layer. Presumably, these large structures are responsible for the increased mixing in the downstream section of the duct, and hence the increased aerodynamic performance observed at NPR=3.4.

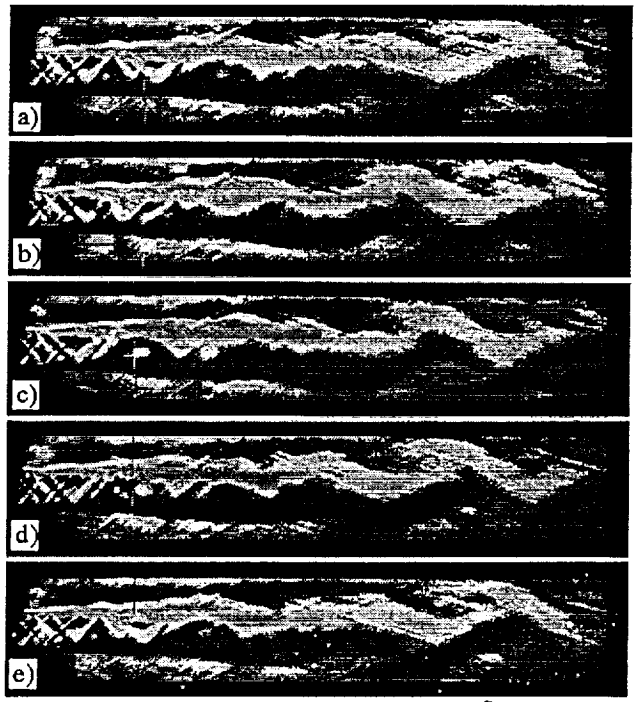

Fig.9 Averaged phase-locked schlieren photographs at various phase angles, unheated (θ=1.0) NPR=3.4 (resonance), a) $\phi=0^{\circ}$, b) $\phi=90^{\circ}$,c) $\phi=180^{\circ}$, d) $\phi=270^{\circ}$, e) $\phi=360^{\circ}$.

In Figure 10, a shadowgraph of the heated jet ejector case (θ=2.2) is shown. This photograph, which shows a lack of the dominant sinuous waves that were observed in Fig.8(a), is typical of the heated primary jet operating in the pressure ratio range 2.0<NPR<5.0.

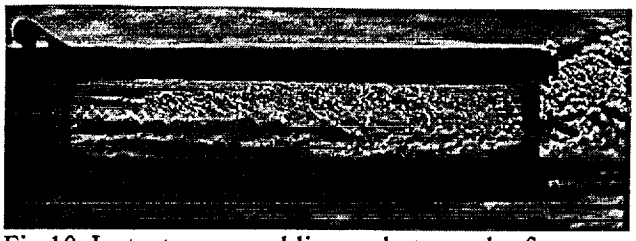

Fig.10 Instantaneous schlieren photograph of heated ejector flowfield (θ=2.2), NPR=3.4.

3.3 Particle Image Velocimetry Measurements

In order to investigate the development of the mixing layer in the internal supersonic region of the ejector, PIV measurements were made in the central XY plane. In Figures 11(a) and 11(b), two multiple-exposed PIV images are shown that correspond to the jet operating

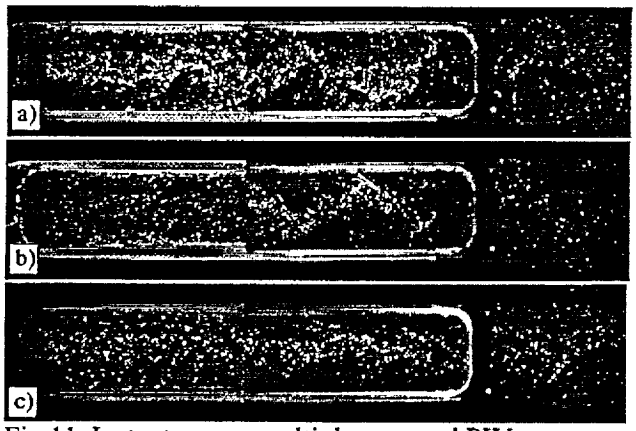

Fig.11 Instantaneous multiple-exposed PIV images of unheated ejector flowfield (θ=1.0), a) NPR=3.4 (resonance), ϕ=0°, b) NPR=3.4 (resonance), ϕ=180°, c) NPR=3.7.

under resonant conditions (NPR=3.4), with the second image 180° out of phase with respect to the first. The bright regions indicate a strong concentration of tracer particles in the primary jet. In Figure 11(c), the image is captured at NPR=3.7 where the jet core extends to the duct exit. Figures 12(a) and 12(b) depict processed instantaneous velocity fields that correspond to the raw data of Figures 11(a) and 11(b), respectively. The sinuous motion observed in the flow-visualization pictures is also observed in the PIV data.

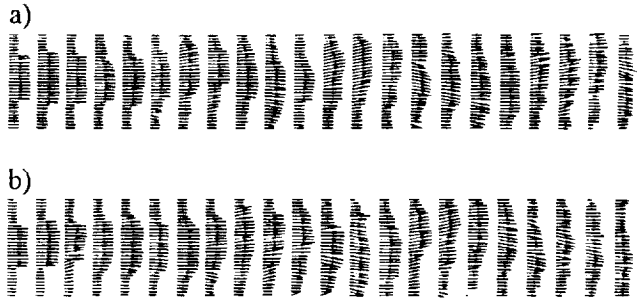

Fig.12 Instantaneous velocity field of unheated ejector flowfield (θ=1.0), a) NPR=3.4, ϕ=0°, b) NPR=3.4, ϕ=180°.

Averaged velocity fields at the two selected NPR's are plotted in Fig.13 in order to directly compare the structure of the ducted primary jet operating under resonance to that of a typical case of the ducted jet operating in the absence of resonance. In Fig.13(a), the presence of resonance results in a clear improvement in the spread of the primary jet inside the duct in comparison to Fig.13(b) where resonance was not present. Despite the relatively small change in primary jet operating pressure, the length of the potential core in Fig.13(a) was significantly reduced by the increased mixing. This is evident by the rapid evolution of the initial "top-hat" profiles into parabolic profiles, and by the flatter velocity profiles at the exit of the duct. The differences in the exit velocity profiles between the two cases are identical to those differences seen in the corresponding Mach number profiles (Fig.6).

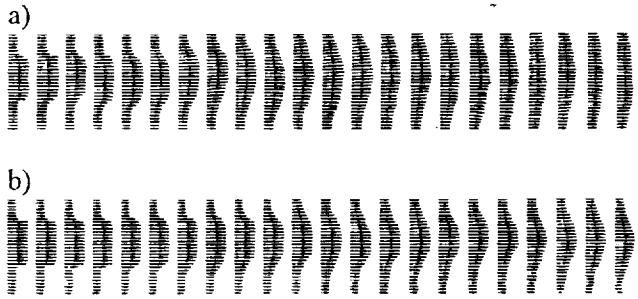

Fig.13 Averaged (15 samples) velocity field of unheated ejector flowfield (θ=1.0), a) NPR=3.4, b) NPR=3.7.

The centerline velocities of the primary jet are plotted from the averaged data in Fig.14. In addition, the centerline velocities of the corresponding unconfined free-jets (at the same NPR's) are included for comparison. As previously stated, the presence of the ejector shroud and associated high-speed secondary entrainment velocity results in a marked reduction in the mixing of the NPR=3.7 ejector case in comparison to the corresponding free-jet. In sharp contrast, duct resonance results in a rapid decay of the average centerline velocity, exceeding even the decay of the corresponding free-jet.

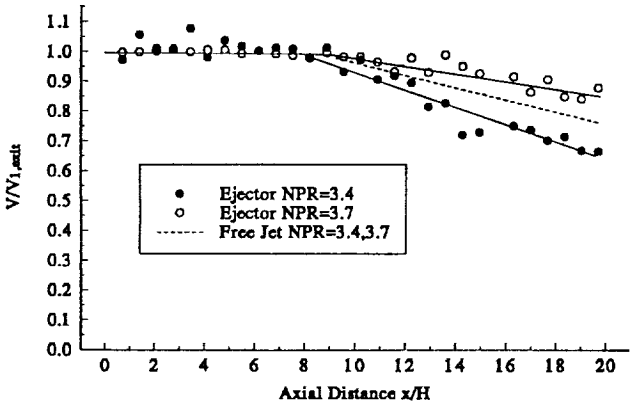

Fig.14 Centerline velocity profiles of unheated ejector and free-jet flow-fields (θ=1.0).

In order to examine the effect of increasing primary jet temperature on the behavior of the internal mixing region, the total temperature of the primary jet was increased and the corresponding velocity fields measured. The velocity plots in Fig.15 correspond to the two primary jet temperature ratios of θ=1.8 and θ=2.2, or T_{01}=525 and T_{01}=650, respectively. In the heated cases, the velocity

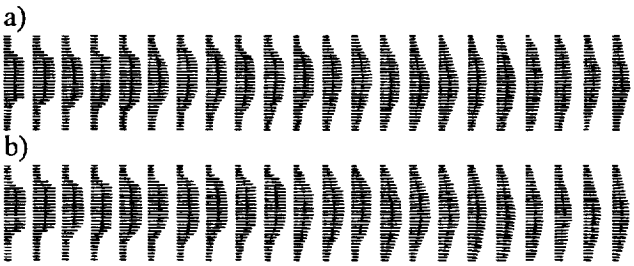

Fig.15 Averaged (15 samples) velocity field of heated ejector flowfield, a) θ=1.8, b) θ=2.2.

profiles at the exit appear unmixed in the absence of resonance. However, the measured secondary mass flow has increased with temperature. This is a result of increasing density and velocity ratios between the primary and secondary streams, an expected result for such mixing layers.[14]

3.4 Internal Primary Jet Shear Layer Growth Rates

A great deal of information is available in the literature concerning the development of confined planar shear layers with constant static pressure boundaries.[14-16] However, the internal development of a confined shear layer in the presence of a strong pressure gradient, such as that found in the present experiment (see Fig.3), is relatively unknown. To determine the effect of the strong pressure gradient on the development of the internal mixing region, the growth rates were measured directly from the averaged whole-field velocity measurements taken inside the ejector duct.

The shear layer thickness used here is based on velocity, in contrast to a definition based on pitot pressure, as normally found in the literature.[14] Similar to the pressure based definition, the thickness used here is defined as the distance between two points in the shear layer where the local velocity is $0.05(V_1-V_2)$ and $0.95(V_1-V_2)$, respectively. It was estimated that the thickness based on pressure and velocity definitions would differ by less that 10% for the range of parameters tested, within the measurement error stated by most authors when estimating shear layer thickness from pressure surveys.[14,16,17] The measured growth rate δ_c' is normalized by the incompressible shear layer thickness δ'_{inc} as proposed by Papamoschou and Roshko [14]. The convective Mach number for each case is defined by:

$$M_c = \frac{V_1 - V_2}{a_1 + a_2}$$

Table 1 contains data from the present experiment including calculated convective Mach numbers and incompressible growth rates.

In order to directly compare a pitot-based and velocity-based measurement of shear layer thickness in the present experiment, the shear layer growth rate was measured using a pitot survey for the unheated rectangular free-jet operating at NPR=3.7. The measured pitot

Test Case	V_1 (m/s)	V_2 (m/s)	a_1 (m/s)	a_2 (m/s)	δ'_{inc}	M_c	δ_c'/δ'_{inc}
A: Free Jet,θ=1.0 NPR=3.4	430	0	288	344	0.26	0.68	0.36
B: Free Jet,θ=1.0 NPR=3.7	430	0	288	344	0.25	0.68	0.36
C: Ejector,θ=1.0 NPR=3.4	**430**	**198**	**288**	**333**	**0.10**	**0.37**	**0.81**
D: Ejector,θ=1.0 NPR=3.7	**430**	**184**	**288**	**334**	**0.11**	**0.40**	**0.49**
E: Ejector, θ=1.8 NPR=3.4	569	204	387	332	0.137	0.51	0.47
F: Ejector, θ=2.2 NPR=3.4	625	206	425	332	0.151	0.55	0.32

Table 1: Experimental Results from PIV data and Isentropic Calculations.

pressure growth rate of $\delta_c'=0.10$ corresponds to the identical velocity-based measurement of $\delta_c'=0.09$, giving confidence to the normalizations and approximations used in the velocity-based measurement of shear layer growth. Also, the lower value obtained in the velocity-based measurement indicates the growth rates based on the shear layer velocity profiles may be underpredicted by comparison to other published results.

With the exception of NPR=3.4 case (C) where resonance is occurring, all data in Table 1 compare well to previous published data (within the band of experimental uncertainty). In observing the ejector cases (D,E,F), the positive pressure gradient imposed on the flow has no apparent effect on the growth of the internal mixing layer. In these experiments, it appears that the static pressure field present in the ejector is the result of increased mixing and not the cause of increased mixing.

However, in the unheated confined flow where resonance is occurring (C), an unusually large growth rate is observed in the mixing layer. The unheated primary jet-ejector was compared at the pressure ratios of NPR=3.4 and 3.7 in order to show the effect of resonance-induced mixing independent of velocity ratio and density ratio effects. Referring again to Table 1, there is only a nominal difference in the values of u_1/u_2, ρ_1/ρ_2 , and M_c between case C and D, but the growth rate of the NPR=3.4 case (C) exceeds that of the NPR=3.7 case (D) by almost 80%. This confirms the fact that the dramatic increase in mixing in the NPR=3.4 jet-ejector case is a result of the fluid-acoustic interaction occurring at that specific pressure ratio, and not an effect of changing convective Mach numbers, velocity ratios, or density ratios.

When resonance is not present, the spread rate data obtained in this ejector study corresponds well with published planar shear layer investigations. This indicates that these analysis techniques can be applied toward the study of confined rectangular free-jets in rectangular ejectors.

4.0 Conclusions

Several aspects of the internal mixing region of a rectangular jet-ejector were investigated. First, the performance gain obtained when the most unstable Strouhal number of the primary jet matched a transverse duct mode was quantified. Mixing increases between the primary and secondary streams were observed when the primary jet was resonating at the first transverse duct mode. Resonance only occurred in the unheated primary jet ejector around one pressure ratio for the entire range tested. As expected, the mixing increase obtained while operating under these conditions resulted in a corresponding improvement of both secondary entrainment and thrust augmentation.

Secondly, the effect of increasing the primary jet temperature on ejector mixing performance was addressed. Increasing the temperature of the primary jet

resulted in a corresponding increase in the performance of the ejector. The behavior of the heated primary jet mixing region was accurately described by the published shear layer growth curves, with the increased convective Mach number of the heated cases resulting in corresponding increases in physical growth rates and mixing.

The absence of resonance in the heated cases is believed to be a result of a frequency mismatch between the most excited mode of the heated primary jet and the duct mode. Assuming the basic parameter describing the conditions of resonance has the form of a Strouhal number, the instability frequency of the jet would shift to a higher value as the primary jet temperature (and velocity) is increased. For this reason, a variable area-ratio ejector is being constructed in an attempt to "tune" the transverse duct mode to the instability frequency of the jet. With the combination of a high-temperature jet-ejector and passive resonance operation, the required shroud length of a realistic heated jet-ejector would be reduced.

Acknowledgments

This work was supported by the NASA Langley Research Center under grant number NAG-1-1497 as part of the ongoing work in the High Speed Research Program.

References

[1] Borchers, I.U., H.J. Hackstein, and P. Bartels, "Study Results on Combat Aircraft Source Noise Reduction", Combat Aircraft Noise, AGARD CP-512, April 1992.

[2] Quinn, B., "Thrust Augmenting Ejectors: A Review of the Application of Jet Mechanics to V/STOL Aircraft Propulsion", Fluid Dynamics of Jets with Applications to V/STOL, AGARD CP 308, November 1981.

[3] Bevilaqua, P.M., "Advances in Ejector Thrust Augmentation", Recent Advances in Aerodynamics; Eds: A. Krothapalli, an C.A. Smith, Springer-Verlag, 1986, pp 375-406.

[4] Krothapalli, A., Ross, C., Yamomoto, K., and Joshi, M.C., "Fluid-Acoustic Interactions in a Low Area Ratio Supersonic Ejector", AIAA Paper No 93-4346, 15th AIAA Aeroacoustic Conference, Oct 1993

[5] Hsia, Y., Krothapalli, A., and Baganoff D., "Mixing of an Underexpanded Rectangular Jet Ejector", Journal of Propulsion, Vol.4, No.3, May-June 1988, pp. 256-262.

[6] Krothapalli, A., Iyengar, K., King, J., a Parekh, D.E., "Sound Generation from a Supersonic Rectangular Jet Ejector", AIAA Paper No. 92-02-108, May, 1992.

[7] Quinn, B., "Effect of Aeroacoustic Interactions on Ejector Performance", Journal of Aircraft, Vol.12, No.11, November 1975, pp 914-916.

[8] Ross, C.B., Lourenco, L., and Krothapalli, A., "Particle Image Velocimetry Measurements in a Shock-Containing Supersonic Flow", AIAA Paper No. 94-0047, 32nd Aerospace Sciences Meeting, Jan 1994.

[9] Lourenco, L.M., Krothapalli, A., and Smith C.A., "Particle Image Velocimetry", Advances in Fluid Mechanics Measurements, Editor: M. Gad-el-Hak, Springer-Verlag, 1989, pp 128-199.

[10] Wishart, D., "Structure of a Heated Supersonic Axisymmetric Jet", Ph.D Dissertation, Florida State University, September 1994.

[11] Quinn, B., "Ejector Performance at High Temperatures and Pressures", Journal of Aircraft, Vol.13, No.12, Dec. 1976, pp. 948-954.

[12] Donovan A.F., and Lawrence, H.R., ed, "High Speed Aerodynamics and Jet Propulsion: Aerodynamic Components of Aircraft at High Speeds", Princeton University Press, 1957.

[13] Krothapalli, A., Van dommelen, L., and Karamcheti, K., "The Influence of Forward Flight on Thrust Augmenting Ejectors", AIAA Paper No. 85-1589, July, 1985.

[14] Papamoschou, D., and Roshko, A., "The Compressible Turbulent Shear Layer: an Experimental Study", Journal of Fluid Mechanics, Vol.197, 1988, pp. 453-477.

[15] Gruber, Mark R., Nathan L. Messersmith, J. Craig Dutton, "Three-Dimensional Velocity Field in a Compressible Mixing Layer", AIAA Journal, Vol.31, No.11, November 1993, pp.2061-2067.

[16] Clemens, N.T., M.G. Mungal, "Two- and Three-Dimensional Effects in the Supersonic Mixing Layer", AIAA Journal, Vol.30, No.4, April 1992, pp.973-981.

[17] Hall, J.L., P.E. Dimotakis, and H. Rosemann, "Experiments in Nonreacting Compressible Shear Layers", AIAA Journal, Vol.31, No.12, December 1993, pp.2247-2254.